Acta Crystallographica Section B
Structural Science
ISSN 0108-7681

A neutron diffraction study of xylitol: derivation of mean square internal vibrations for H atoms from a rigid-body description

Anders Østergaard Madsen,[a] Sax Mason[b] and Sine Larsen[a]*‡

[a]Centre for Crystallographic Studies, Department of Chemistry, University of Copenhagen, Universitetsparken 5, DK-2100 København, Denmark, and [b]Institut Laue–Langevin, 6 rue Jules Horowitz, BP 156 38042 Grenoble CEDEX 9, France

‡ Present address: European Synchrotron Radiation Facility, 6 rue Jules Horowitz, BP 220, F-38045 Grenoble CEDEX, France.

Correspondence e-mail: sine@ccs.ki.ku.dk

Received 14 March 2003
Accepted 21 July 2003

A neutron diffraction study of xylitol ($C_5O_5H_{12}$) is presented. The nuclear anisotropic displacement parameters have been analysed showing that the carbon–oxygen skeleton conforms to a rigid-body (TLS) description. Applying this TLS model to the xylitol H atoms allows characterization of the internal molecular displacements of the H nuclei, assuming that the observed H nuclear mean-square displacements are a sum of the internal displacements and rigid-body displacements. These internal molecular displacements are very similar for chemically equivalent H atoms and in good agreement with the values obtained by other methods. In all cases the smallest eigenvector of the residual mean-square displacement tensor is almost parallel to the X—H bond. The use of *ab initio* calculations to obtain the internal vibrations in xylitol is discouraging. Another 12 structures extracted from the literature which have been investigated by neutron diffraction were subjected to a similar analysis. The results for the nine compounds investigated at low temperature conform to the results from xylitol and provide estimates of the internal vibrations of H atoms in a range of chemical environments.

1. Introduction

Modeling parameters for H atoms is a non-trivial problem in experimental charge density studies that are based solely on X-ray diffraction data. Nevertheless, a good estimate of these parameters is crucial for the deconvolution of a static charge density model from the thermally smeared charge density.

Supplementing the study with a neutron diffraction experiment is not always a possibility because of difficulties in growing crystals of sufficient size and the limited availability of neutron sources. In order to overcome the shortage of reliable parameters for H atoms derived from a neutron diffraction experiment, different approaches have been employed in studies of experimental charge densities.

The apparent shortening of bond lengths involving H atoms observed in X-ray compared with neutron diffraction studies is compensated by changing the position of the H atoms. The direction of the bond is maintained, but the bond is elongated to match the bond lengths derived from neutron diffraction studies. To determine the atomic displacement parameters for the H atoms in experimental charge density studies many investigators use the easy solution of modelling the thermal motion of the H atoms by assuming an isotropic displacement, although it is obvious that this is a highly inadequate model.

Another approach which has been employed with apparent success is to estimate the hydrogen anisotropic displacement parameters (ADPs) as a combination of rigid-body motion and internal vibrations, making use of the assumption that the

internal vibrations and rigid-body movements are uncorrelated (Higgs, 1955).

The rigid-body motion can be obtained by refining a (segmented) rigid-body model to the non-H atom ADPs, while the internal vibrations are assigned on the basis of 'spectroscopic evidence' (Hirshfeld & Hope, 1980; Destro & Merati, 1995), derived from *ab initio* calculations (Flaig *et al.*, 1998) or assigned on the basis of rigid-body analyses of similar compounds studied by neutron diffraction (Chen & Craven, 1995).

In these studies it was assumed that spectroscopic measurements support the assumption that the internal vibrations for H atoms in similar chemical groups are of comparable magnitude.

A number of studies based on neutron diffraction data have investigated the deviations from the rigid-body model of the ADPs for the H atoms by analysis of residual mean-square displacements, $U_{obs} - U_{calc}$, where U_{calc} represents the parameters from the rigid-body model. First, Johnson (1970) showed that plausible estimates of C—H and C—D vibration amplitudes could be obtained by analysis of the non-H skeleton of hydrocarbon derivatives. More recently, Craven and co-workers have analysed the mean-square displacements (MSDs) in cholesteryl acetate (Weber *et al.*, 1991), suberic acid (Gao *et al.*, 1994), hexamethylene tetramine (Kampermann *et al.*, 1995) and piperazinium hexanoate (Luo *et al.*, 1996).

These studies showed that the chemically equivalent C—H bonds have remarkably similar internal MSDs over a range of temperatures and that the differences between the C—H and C—D internal MSDs are in accordance with the difference in mass of the corresponding two-atomic harmonic potential.

The work presented here follows in the footsteps of these investigators. In order to establish an accurate set of hydrogen nuclear parameters for xylitol, a pentitol epimer, we have collected low-temperature [122.4 (5) K] neutron diffraction data.

A rigid-body model has been obtained by analysis of the C and O ADPs. The model was subsequently used to obtain estimates of the H-atom internal MSDs by subtraction from the hydrogen ADPs.

In order to examine the general nature of the results obtained from our investigations of xylitol we have conducted a similar analysis for 12 other molecular crystals where neutron diffraction data were available. The neutron diffraction data were collected at temperatures in the range 20–293 K, the compounds were selected on the criteria that they should be comprised of light atoms (suitable for a charge-density study) and that ADPs should be available.

2. Experimental and computational aspects

2.1. Crystallization of xylitol

Xylitol, purchased from Sigma, was recrystallized from ethanol (95%) by slow evaporation. The rate of evaporation controls the size of the crystals. The best results are obtained by keeping the solution at room temperature.

2.2. Data collection

Several crystals were tested in order to select the most suitable crystal for the data collection. A many faceted prismatic colourless transparent crystal was selected (approximately 5.5 mm^3) and glued to a vanadium pin using a two-component glue (Kwikfill). It was mounted on the Eulerian cradle of the neutron four-circle diffractometer D9 at the ILL reactor. The instrument was equipped with a two-stage Displex cryorefrigerator, which was used to cool the crystal to 122.4 K (RMSD 0.041 K, min/max 122.1/122.8 K) during the experiment, and with a 32 × 32 pixel position-sensitive detector. A Cu (220) monochromator in transmission geometry was used to select a neutron beam of wavelength 0.8395 (1) Å. The sample was slowly cooled (3 K min^{-1}) while monitoring a strong reflection. No splitting or change in mosaicity of the crystal was observed.

Intensity data [$(\sin\theta/\lambda)_{max} = 0.84$ $Å^{-1}$] were measured by means of coupled ω–$x\theta$ scans with a scan width between 1.2 and 4.5° and x values between 1 and 2. The initial measuring time of *ca* 5 s per step (30 000 monitor counts/pnt, 30 points) was increased to *ca* 10 s (60 000 monitor counts/pnt) for the weaker data.

During the data collection two strong reflections (−2 8 0 and 3 0 7) were measured every 100 reflections and their intensities displayed no significant or systematic variations.

D9 was operating with thermal neutrons so the contribution from shorter wavelengths was marginal and no significant $\lambda/2$ component was observed. In all, 2917 reflections were collected and integrated in three-dimensions using the ILL program *RACER* (Wilkinson *et al.*, 1988). The final unit cell (Table 1) was determined by a least-squares fit to all the significant collected reflections using the ILL program *RAFD*9 (Filhol, 1987).

2.3. Data reduction

Three ψ scans (F^2 as a function of the ψ angle) of the −4 4 1, −4 3 3 and −4 3 1 reflections showed that an absorption or extinction correction was necessary.

Absorption cross sections at 1.798 Å tabulated in Sears (1992) were scaled linearly to the experimental wavelength. The attenuation coefficients were used as tabulated for C and O, while values (a sum of the incoherent scattering and true absorption cross section) for hydrogen based on measurements at ILL by Frost and Mason (personal communication) were used. The resulting attenuation coefficient was 2.707 cm^{-1}. The absorption correction was performed with the ILL version of the program *DATAP* (Coppens *et al.*, 1965) and this correction significantly improved the statistics of merging equivalent measurements, mainly because the ψ-scan reflections were included in the average ($R_{int}^{before} = 6.16\%$, $R_{int}^{after} = 4.10\%$ for all reflections). After merging in the point group *mmm* with the program *SORTAV* (Blessing, 1987), 1911 independent reflections remained.

Table 1
Experimental table.

Crystal data	
Chemical formula	$C_5H_{12}O_5$
M_r	152.15
Cell setting, space group	Orthorhombic, $P2_12_12_1$
a, b, c (Å)	8.2660 (4), 8.8977 (4), 8.9116 (4)
V (Å^3)	655.43 (5)
Z	4
D_x (Mg m^{-3})	1.540
Radiation type	Neutron
No. of reflections for cell parameters	2917
θ range (°)	3.8–45.3
μ (mm^{-1})	0.27
Temperature (K)	122.4 (4)
Minimum/maximum temperature (K)	122.1/122.8
Crystal form, colour	Prism, colourless
Crystal size (mm)	2.5 × 2.0 × 0.9
Data collection	
Diffractometer	Four-circle
Data collection method	ω–$x\theta$, $1 \leq x \leq 2$
Scan width (°)	1.2–4.5
Scan time	5–10 s per step
Absorption correction	Integration
T_{min}	0.5415
T_{max}	0.6955
No. of measured, independent and observed reflections	2917, 1911, 1831
Criterion for observed reflections	$I > 2\sigma(I)$
R_{int}	0.041
θ_{max} (°)	45.3
Range of h, k, l	$-13 \Rightarrow h \Rightarrow 3$ $-3 \Rightarrow k \Rightarrow 15$ $-5 \Rightarrow l \Rightarrow 10$
No. and frequency of standard reflections	2 every 100 reflections
Intensity decay (%)	0
Refinement	
Refinement on	F^2
$R[F^2 > 2\sigma(F^2)]$, $wR(F^2)$, S	0.0531, 0.054, 1.47
No. of relections	1911
No. of parameters	200
H-atom treatment	Refined independently
Weighting scheme	Based on measured s.u.'s $w = 1/\sigma^2(F_o^2)$
$(\Delta/\sigma)_{max}$	<0.0001
$\Delta\rho_{max}$, $\Delta\rho_{min}$ (e Å^{-3})	1.81, −1.23
Extinction method	Becker–Coppens type 1 isotropic Lorentzian
Extinction coefficient	12 892 (154)

Computer programs: *RAFD*9 (Filhol, 1987), *RACER* (Wilkinson *et al.*, 1988), *DATAP* (Coppens *et al.*, 1965), *SHELXL* (Sheldrick, 1990), *VALRAY* (Stewart *et al.*, 2000), *ORTEP*II (Johnson, 1976), *PLATON* (Spek, 1990).

2.4. Structure refinement

VALRAY (Stewart *et al.*, 1998) was used for the full-matrix least-squares refinement based on all reflections, minimizing $\sum w_{\bar{h}}[|F_o(\bar{h})|^2 - k|F_c(\bar{h})|^2]^2$, with weights $w = 1/\sigma^2[|F_o(\bar{h})|^2]$ based on counting statistics. The initial atomic coordinates were taken from the X-ray structure determination (Kim & Jeffrey, 1969) and the neutron scattering lengths used were $b_c(\mathrm{C}) = 6.646$, $b_c(\mathrm{O}) = 5.803$ and $b_c(\mathrm{H}) = -3.739$ fm (Sears, 1992).

An isotropic extinction parameter (Becker & Coppens, 1975) was included in *VALRAY* [g = 0.000129 (2) rad^{-1}, $(F_{obs}/F_{cor})_{min} = 0.624$ for the 0 1 5 reflection]. The 200 parameters varied during the refinement comprised the extinction parameter, scale factor, and positional and anisotropic displacement parameters for all atoms. Details are given in Table 1 and the refined nuclear parameters have been deposited.[1]

2.5. Theoretical calculations

To achieve an estimate of the internal nuclear motion for xylitol in the crystalline state, single-molecule geometry optimizations at the DFT B3LYP/6-311G(d,p) level[2] were performed, starting at the molecular geometry observed in the crystal.

Although the energy and forces between atoms readily converge, large geometrical differences were still seen between subsequent optimization steps, indicating that the molecule has a very flat potential energy surface. In order to achieve convergence it was necessary to impose very tight criteria for the forces: a threshold of 2×10^{-6} and 1×10^{-6} a.u. for the maximum and r.m.s. force, respectively. The GDIIS optimization algorithm, recommended for structures with very flat potential energy surfaces, was used. Without employing this algorithm we were unable to obtain convergence.

The automated procedure in *Gaussian*98 (Frisch *et al.*, 1998) was used to calculate the frequencies and the corresponding normal mode eigenvectors of displacement for the geometry-optimized xylitol molecule. Subsequently, the result was transformed to mean-square displacements using the procedure outlined in *Appendix A*.

3. Results and discussion

3.1. Analysis of the atomic displacement parameters

The atomic labelling of xylitol and the displacement parameters obtained by the refinement from the neutron diffraction data are shown in Fig. 1. The overall molecular geometry of xylitol is in excellent agreement with the results from the previous X-ray diffraction study by Kim & Jeffrey (1969). The ADPs can be validated by the 'rigid-bond test' formulated in 1972 by Hirshfeld, implying that physically realistic ADPs should be reflected in small differences (≤ 0.001 Å^2) in mean-square displacements of the bonding atoms in the direction of the bond.

The 'rigid-bond test' conducted for the C—C and C—O bonds gives an average $\Delta(U_{bond})$ difference of 0.0004 Å^2 with C3—O3 being the only one outside the accepted range with $\Delta(U_{bond})$ = 0.0017 Å^2, which shows that ADPs obtained for xylitol are of a quality that merits a rigid-body analysis.

Examination of the non-bonded intramolecular $\Delta(U)$s is important in order to establish whether torsional motion in the framework can be neglected. The r.m.s. of the non-bonded

[1] Supplementary data for this paper are available from the IUCr electronic archives (Reference: BS5000). Services for accessing these data are described at the back of the journal.
[2] Several other minor basis sets have been tested using DFT and HF theory, but with qualitatively the same results.

$\Delta(U)$'s is 0.0012 Å^2. The largest component in this sum is Δ(O3—O4) of 0.0032 Å^2. Although these values are higher than acceptable by the rigid-bond postulate, they are much lower than values found in truly non-rigid systems (Dunitz *et al.*, 1988; Rosenfield *et al.*, 1978). Indeed, the incorporation of torsional librations (Schomaker & Trueblood, 1998) about the C3—C4 and C3—C2 axes in the model leads to librations that are barely significant.

Using the *THMA*11 program (Schomaker & Trueblood, 1968) a TLS rigid-body model was obtained from a least-squares fit to the ADPs of the C and O atoms. The least-squares weights were based on the experimental standard deviations of the ADPs. The overall agreement parameters used in the *THMA*11 program (defined in *Appendix B*) show that this model provides a good description of the ADPs for carbon and oxygen [$wR(U_{ij})$ = 0.115]. The r.m.s.($w\Delta U$) is 0.0008 Å^2.

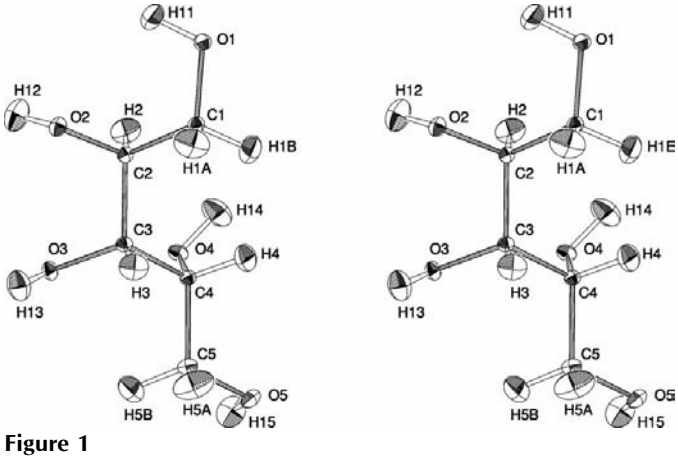

Figure 1
Stereo *ORTEP*II (Johnson, 1976) plot of the total mean-square displacements derived from the xylitol neutron diffraction experiment. The ellipsoids are shown at the 50% probability level.

The discrepancy from the rigid-body model is visualized in Fig. 2 using the *PEANUT* program (Hummel *et al.*, 1990), which displays the differences between the observed ADPs and those calculated from the rigid-body model. The *PEANUT* plots in this paper show root-mean-square displacements (RMSDs). The positive part of the RMSD surfaces are represented by solid lines and the imaginary part (corresponding to negative mean-square displacements) are shown as dotted surfaces. The scale of the RMSD surfaces is 1.54 in all illustrations.

It is apparent from Fig. 2(*a*) that the rigid-body model provides a satisfactory description of the atomic displacements for the C and O atoms, but cannot account for atomic displacements of the H atoms. Indeed a model fitted to all atoms in xylitol refines to $wR(U_{ij})$ = 0.405 with an r.m.s. of the weighted $\Delta(U)$ of 0.0038 Å^2. An inspection of Fig. 2(*a*) reveals, however, that chemically equivalent H atoms have similar features in the *PEANUT* plots and that the largest discrepancy from the rigid-body model for the H atoms is almost perpendicular to the covalent bond. These observations initiated further investigations of differences between the observed (experimental) displacement parameters for the H atoms and those obtained from a rigid-body model based on the non-H atoms.

3.2. Analysis of the residual ADPs

Our initial aim in the analysis of the residual ADPs was to examine whether they reflect the expected internal vibrations of the H atoms. To conduct this analysis the observed differences $U_{obs} - U_{cal}$ were converted into a Cartesian coordinate system followed by a diagonalization of the resulting 3×3 tensor.

The program written to perform these calculations can also compare the directions of the eigenvectors with a local coor-

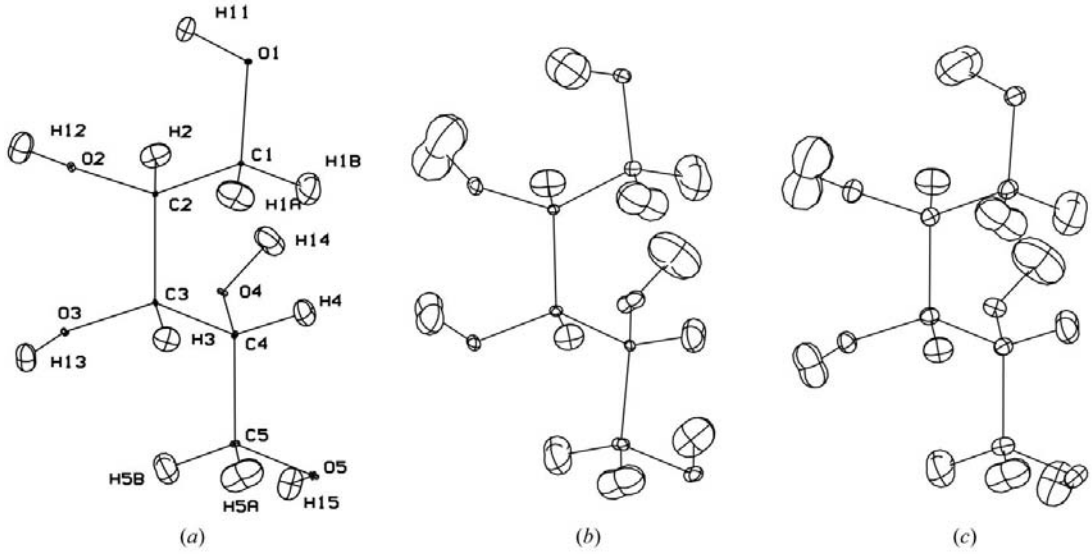

Figure 2
PEANUT (Hummel *et al.*, 1990) plots of RMSD surfaces for xylitol RMSDs scaled up by 1.54. (*a*) Neutron experiment TLS refinement difference surface ($U_{obs} - U_{calc}$). (*b*) Geometry-optimized configuration showing the mean-square displacements corresponding to the vibrational frequencies calculated by *Gaussian*98 (Frisch *et al.*, 1998). (*c*) H atoms: theoretical mean-square displacements transformed to the *crystal* geometry, C and O atoms: total *experimental* mean-square displacements.

Table 2
Analysis of residual root-mean-square displacements (10^{-4} Å^2) from the TLS analysis of the xylitol neutron diffraction experiment.

The total and residual MSDs in the X—H direction and the U_{iso} value calculated as suggested by Stewart (1975) are listed in the section to the left. The eigenvalues of the residual MSD matrix are listed with the angle between the corresponding eigenvector and the closest axis in the local atomic coordinate system.

Eigenvalues of the residual MSD matrix									
	$\langle\mu\rangle$ in X-H direction			Bond direction		Out-of-plane		In-plane	
	Residual	Total	U_{iso}	Angle	Value	Angle	Value	Angle	Value
H1*A*	45 (8)	145	252	12.3	36	9.2	172	8.3	308
H1*B*	51 (10)	146	250	10.0	43	2.8	152	10.4	339
H5*A*	54 (10)	142	279	12.1	38	2.2	158	12.3	404
H5*B*	77 (8)	189	251	19.4	48	3.1	132	19.7	309
H2	54 (7)	130	198	7.8	52	34.0	201	34.5	111
H3	51 (7)	120	195	6.6	50	35.0	147	34.4	129
H4	43 (6)	123	204	5.0	42	5.9	150	6.5	167
H11	34 (9)	129	208	14.7	23	14.9	184	3.2	132
H12	88 (8)	165	240	14.0	82	16.5	220	15.6	118
H13	56 (6)	157	214	4.5	56	24.3	181	24.0	71
H14	55 (9)	145	235	19.2	44	12.1	256	22.8	146
H15	42 (8)	153	230	12.1	34	11.7	219	3.0	107

dinate system defined with one axis parallel to the X—H bond, another perpendicular to a plane defined by the closest H, C or O atoms (out of plane), and the third (in plane) completing the right-handed orthogonal system. An example of a result of this analysis is illustrated by the *PEANUT* drawing in Fig. 3 showing the mean square displacements for C4, O4 and H14, along with the local coordinate system used to define the bond in the in-plane and out-of-plane directions and the eigenvectors of the residual mean-square displacement matrix of the H14 atom. The overall results of this analysis are presented in Table 2. First, it should be noted that for all the H atoms the smallest eigenvalue corresponds to the eigenvector directed towards the X—H bond. We have used the relation between the mean-square displacement and the associated frequency based on a quantum statistical approach (*e.g.* Willis & Pryor, 1975) to estimate the frequencies associated with the displacements

$$\langle u^2\rangle = \frac{h}{4\pi^2 m\nu}\left(\frac{1}{2}+\frac{1}{e^{h\nu/k_{\rm B}T}-1}\right). \quad (1)$$

Here $\langle u^2\rangle$ is the mean-square displacement, m is the reduced mass of the harmonic oscillator and ν is the frequency.

The residual mean-square displacements in the bond directions are in the range 0.0034 (9)–0.0088(8) Å^2. O—H stretching frequencies are typically 3700 cm^{-1} and C—H frequencies are 2850 cm^{-1}, which correspond to mean-square displacements of 0.0048 and 0.0064 Å^2 (1) in good accordance with the values from the mean-square displacements. Similarly the in-plane mean-square displacement of the terminally bonded H atoms (CH_2) has a CH_2 rocking frequency of *ca* 720 cm^{-1} (0.0253 Å^2) as a major contributor. The mean-square displacements of H2, H3 and H4 are also in accordance with the C—H bending motion (frequency 1340 cm^{-1} $\sim$ 0.0135 Å^2). The oxygen-bound H atoms have very similar vibrations, although the out-of-plane MSDs are somewhat larger than the typical O—H bending motion (1410–1260 cm^{-1} $\sim$ 0.0126–0.0141 Å^2).

3.3. Comparison with equivalent isotropic displacement parameters

We wanted to examine the weaknessess of employing the simple isotropic description of the H-atom displacements. As most of the charge density associated with the covalently bonded H atom is located in the X—H bond region, it is important to compare the mean-square displacement in the bond direction to the anisotropic result.

We have used the approach of Stewart (1975) to estimate the equivalent isotropic displacement parameters. These values of $U_{\rm iso}$ shown in Table 2 are an estimate of values that would have been obtained if the H atoms had been refined with isotropic displacement parameters. While the total mean-square displacement in the bond direction is in the range 0.0120–0.0189 Å^2, $U_{\rm iso}$ values range from 0.0195 to 0.0279 Å^2, with a mean difference of 0.0084 Å^2 showing a significant deviation from mean-square displacements derived from the anisotropic description. This is probably a minimum deviation, as refinement of an isotropic displacement parameter with X-ray data will give an even higher value. The isotropic displacement parameter derived from X-ray analysis depends on the H-atom scattering factor used and the chemical environment. The SDS (Stewart *et al.*, 1965) hydrogen form factor – the *de facto* standard in most small molecule structure refinement programs – has been found to give an increase in the isotropic displacement parameters compared with the neutron analysis result (Stewart, 1975; Coppens *et al.*, 1979).

3.4. Theoretical calculations

In principle, the internal vibrations can be estimated from theoretical calculations. The approach employed by Luo *et al.*

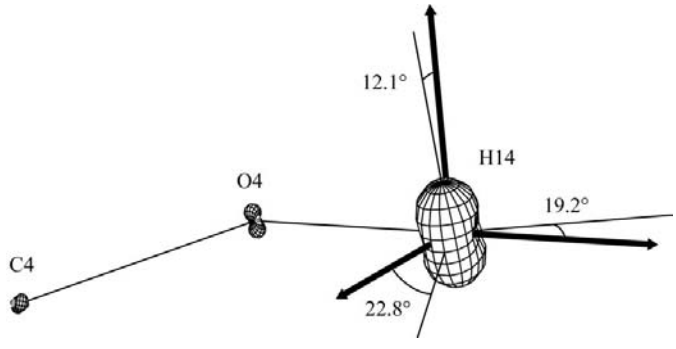

Figure 3
PEANUT (Hummel *et al.*, 1990) plot of the xylitol C4—O4—H14 fragment difference RMSD surface ($U_{\rm obs}-U_{\rm calc}$). RMSDs scaled up by 1.54. The local coordinate system (thick lines) and the eigenvectors of the residual mean-square displacement matrix (thin lines) are indicated.

(1996) and Flaig *et al.* (1998) provides an alternative route to estimate the internal mean-square displacements for the H atoms using single-molecule *ab initio* calculations. Such an independent estimate of the MSD corresponding to internal vibrations is attractive, because the MSD matrices of the atoms used in the rigid-body analysis should be corrected for contributions from internal vibrations. At the temperatures typically used in experimental charge-density analysis (10–120 K) the relative contribution from the internal vibrations to the overall mean-square displacement is considerable even for non-H atoms and becomes larger as the temperature is decreased.

Table 3
Estimate of internal mean-square displacements (10^{-4} Å^2) obtained by theoretical calculations.

	$\langle\mu^2\rangle_{\rm bond}$	$U_{\rm arit}$	Eigenvalues			U^{11}	U^{22}	U^{33}	U^{12}	U^{13}	U^{23}
O1		70	23	59	129	50	99	63	36	−1	30
O2		67	21	40	139	35	81	85	−20	−6	53
O3		52	26	32	97	32	62	62	−10	−13	31
O4		104	25	47	239	56	36	219	−1	48	−37
O5		65	19	54	123	32	42	121	−16	11	9
C1		69	19	31	158	42	119	47	32	20	51
C2		27	19	30	32	20	32	29	0	−4	−1
C3		32	15	36	45	17	36	43	−3	−7	1
C4		30	19	24	48	21	35	36	−2	−5	12
C5		49	19	23	104	24	22	101	−2	−6	16
H1*A*	173	369	89	183	833	445	524	136	337	−20	−93
H1*B*	145	395	77	223	887	205	502	479	−152	−50	365
H2	80	187	79	184	300	191	160	211	27	−17	−102
H3	89	155	89	164	214	164	144	158	11	−1	−61
H4	81	198	77	185	332	214	277	103	−55	−21	73
H5*B*	116	279	84	190	564	210	406	222	−66	−60	209
H5*A*	137	298	74	194	626	187	121	586	25	26	−140
H11	143	430	103	288	898	164	393	732	−115	−35	277
H12	138	623	77	345	1449	669	361	841	−95	672	−93
H13	73	275	69	208	547	216	346	262	−191	−46	132
H14	197	481	83	567	795	649	183	612	222	−121	35
H15	115	297	82	272	536	312	128	450	−45	85	−129

We have tested this approach on xylitol. Details of the calculations are contained in §2.5. The crystal and SCF optimized geometry as well as the resulting atomic mean-square displacements at the B3LYP/6-311G(*d*,*p*) level are compared in the *PEANUT* drawings in Fig. 2(*b*). The carbon–oxygen frame is almost unchanged, confirming that the crystal geometry corresponds to a local minimum in the gas phase. It has been suggested that the bend conformation, a general effect found in alditols, is a consequence of unfavorable 2,4-syndiaxial intramolecular interactions rather than a result of favourable intermolecular interactions (Jeffrey, 1990). A relaxed potential-energy surface scan around the C1—C2—C3—C4 torsional angle calculated at the HF/STO-3G level reveals three local minima. Upon geometry optimization at the B3LYP/6-311G(*d*,*p*) level the minimum closest to the crystal geometry has the highest energy, with an energy difference of 24 kJ mol^{-1} compared with the lowest minima, which does not support the earlier suggestions mentioned by Jeffrey (1990).

The hydrogen positions in the optimized and crystal geometries are significantly different. In the absence of a crystal environment the geometry changes towards forming three (H11···O2 2.433 Å, H13···O2 2.186, H15···O4 2.372 Å) intramolecular hydrogen bonds rather than one (H11···O2 2.4946 Å).

The resulting mean-square displacements (Fig. 2*c* and Table 3) are grossly overestimated, especially for the oxygen-bound H atoms. This stems from the very flat potential energy surface, a consequence of the missing crystal environment. H12 and H14 are not hydrogen bonded and have the largest MSD amplitudes. Only H atoms bound to carbon seem to have reliable MSD estimates. The O4 atom has a larger internal MSD amplitude than the total experimental MSD.

Evidently the procedure does not yield viable estimates of the internal vibrations for xylitol. Similar conclusions were made by Luo *et al.* (1996) for the hexanoate anion, where the calculated in-plane mean-square displacements for H atoms in methylene groups were four to five times higher than the experimental result.

These deviations can be attributed to the missing crystalline environment. Successful attempts have been made to perform *ab initio* calculations incorporating the effect of the crystal field (*e.g.* Rousseau *et al.*, 1998; Capelli *et al.*, 2000); however, it is obvious that these approaches have not yet reached the stage of standard procedures.

4. Extension to other systems

The neutron diffraction results for 12 other structures found in the literature have been investigated by rigid-body analysis. A number of carbohydrate structures have been chosen for comparison with xylitol. These structures have H atoms in hydroxy, methine, methylene and methyl groups. Furthermore, three structures with short hydrogen bonds, water molecules and methylammonium ions have been investigated. The experimental temperatures range from 20 K to room temperature. Table 4 shows the references and TLS refinement statistics (defined in *Appendix B*) for all the structures. Details of the analyses presented here can be found in the supplementary material.

The H atoms in all the structures examined, even those at room temperature, consistently have the smallest eigenvector of the residual MSD matrix closest to the bond direction. For the low-temperature studies, the bond-directed mean square displacements are very similar. Root-mean-square values and associated standard deviations for the different functional groups are compiled in Table 5. These numbers are in good agreement with those reported by Weber *et al.* (1991) and the r.m.s. deviations are smaller, except for the in-plane vibrations in the methyl groups.

Table 4
Refinement statistics for TLS models.

The residuals are defined in *Appendix B*.

Model	Reference	$wR^2(F^2)$	Temperature	$wR^2(U^{ij})$	$wR^2(U^{ii})$	r.m.s.$(w\Delta U)$	e.s.d.$(w\Delta U)$
Methyl α-D-lyxofuranoside	(*a*)	0.1024	20.0 (1)	0.139	0.106	0.0006	0.0007
Methyl α-D-xylofuranoside	(*a*)	0.0853	20.0 (1)	0.134	0.079	0.0006	0.0007
Methyl β-D-arabinofuranoside	(*a*)	0.117	20.0 (1)	0.130	0.084	0.0007	0.0008
Erythritol	(*b*)	0.050	22.6 (5)	0.087	0.057	0.0004	0.0005
Sodium hydrogen maleate trihydrate (maleate ion)	(*c*)	0.059	120 (1.5)	0.032	0.020	0.0003	0.0004
Xylitol		0.0540	122.4 (5)	0.120	0.099	0.0008	0.0010
Methylammonium hydrogen succinate monohydrate†	(*d*)	0.0603	122.4 (5)	0.047	0.032	0.0005	0.0007
Methylammonium hydrogen maleate (anion 1)	(*e*)	0.1081	122.4 (5)	0.019	0.012	0.0003	0.0004
Methylammonium hydrogen maleate (anion 2)	(*e*)	0.1081	122.4 (5)	0.021	0.013	0.0003	0.0004
Alpha-L-xylopyranose	(*f*)	0.042	123 (1)	0.086	0.066	0.0010	0.0012
Beta-L-arabinopyranose	(*f*)	0.031	123 (1)	0.061	0.048	0.0005	0.0006
Potassium-D-gluconate *A* form	(*g*)	0.037‡	298	0.161	0.140	0.0033	0.0038
Potassium-D-gluconate *B* form	(*g*)	0.045‡	298	0.177	0.154	0.0015	0.0017
D-Glucitol	(*h*)	0.032‡	298	0.215	0.156	0.0038	0.0044

References: (*a*) Evdokimov *et al.* (2001); (*b*) Ceccarelli *et al.* (1980); (*c*) Olovsson *et al.* (1984); (*d*) Flensburg *et al.* (1995); (*e*) Madsen *et al.* (1998); (*f*) Jeffrey *et al.* (1980); (*g*) Panagiotopoulos *et al.* (1974); (*h*) Park & Jeffrey (1971). † The TLS analysis of MAHS does not use the mean square displacement matrices reported in Flensburg *et al.* (1995), but rather the result of a preliminary refinement without third- and fourth-order cumulants. ‡ Refinement on *F*: the reported residual is $wR^2(F)$.

Table 5
Mean-square amplitudes (10^{-4} Å^2) for internal vibrations of hydrogen nuclei.

All the low-temperature structures are included in these mean values. The out-of-plane MSDs from alpha-L-xylopyranose and beta-L-arabinopyranose are excluded owing to the suspect negative values.

	No. of $X-$H groups	$X-$H stretch	$X-X-$H out-of-plane	$X-X-$H in-plane	$U_{iso} - U_{bond}$
Methylene	18	51 (11)	145 (33)	246 (72)	86 (32)
Methyl	14	38 (13)	369 (90)	245 (115)	134 (34)
Methine	28	50 (13)	148 (27)	140 (23)	79 (31)
Hydroxy	24	35 (22)	183 (43)	101 (34)	67 (18)
Water	7	54 (27)	174 (70)	157 (74)	85 (17)
Ammonium	5	28 (15)	150 (33)	141 (50)	70 (15)

The rightmost column in Table 5 shows the mean value of the difference between the bond-directed MSD in the isotropic and anisotropic description. The difference reflects the anisotropy of the MSDs, which depend on the temperature and the chemical environment. The largest difference is seen for the H atoms in methyl groups, whose motion is dominated by the very large out-of-plane (methyl torsion) vibrations. The overall mean value for the low-temperature studies is 0.008 (4) Å^2.

The amplitudes of the high-frequency internal vibrations are the least temperature-dependent, so the relative contribution from internal vibrations to the overall atomic mean-square displacement becomes larger as the temperature is decreased. Therefore, in principle, the rigid-body approximation should be best at elevated temperatures. This is, nevertheless, not supported by the results from the room-temperature studies.

The ADPs for the structures resulting from experiments at room temperature have standard uncertainties (s.u.s) approximately five times higher than the low-temperature studies. The s.u.s. are around 0.005 Å^2 for the H atoms and of the same magnitude as the $X-$H stretching vibrations. The models obtained by a TLS analysis contain less precise information than is needed. Although the smallest eigenvector of the residual MSD matrix in most cases is the one closest to the bond direction, the actual eigenvalues are very scattered. Very little information can be gained from such room-temperature structures of limited accuracy and they are consequently not considered any further.

4.1. Carbohydrate structures

The analysis of erythritol (Fig. 4) confirmed our expectations. The structural similarities with xylitol are reflected in the internal vibrations derived from the rigid-body analysis (Table 6). The only obvious difference concerns the methylene in-plane vibrations which are somewhat larger in xylitol. This is discussed further below.

Although the structural likeness between xylitol and the furanosides is small, the same functional groups are present. Three furanosides recently studied by Evdokimov *et al.* (2001) at low temperature have strikingly similar internal vibrations. Fig. 5 illustrates the residual MSDs for the methyl-α-D-xylofuranoside crystal structure. An analysis of these MSDs is given in Table 7. The mean eigenvalues of the bond-directed, in-plane and out-of plane internal vibrations of the methyl groups are 0.0041 (8), 0.0171 (26) and 0.0365 (51) Å^2 for the nine H atoms in these furanosides. The r.m.s. deviation of the eigenvalues associated with the bond direction is much less than one standard uncertainty of the full MSD.

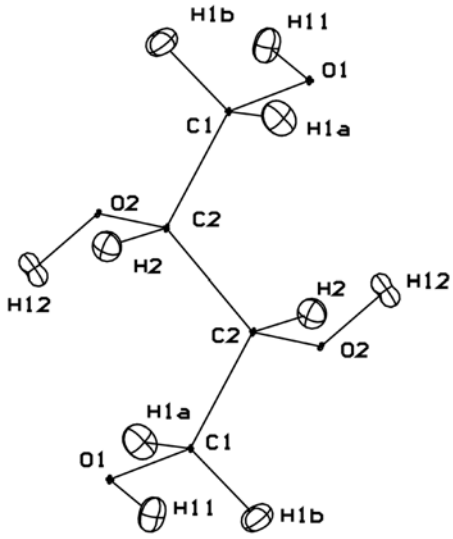

Figure 4
PEANUT (Hummel *et al.*, 1990) plot of the erythritol neutron experiment TLS refinement difference RMSD surface ($U_{obs} - U_{calc}$). RMSDs scaled up by 1.54.

The methylene out-of-plane vibrations are remarkably similar in all the low-temperature structures. The in-plane vibrations, however, show systematic variations. Xylitol and the anion in methylammonium hydrogen succinate monohydrate (MAHS) have displacements 50% larger than the other structures. The residual mean-square displacement of the methylene C atoms in xylitol reveals a small positive residual displacement in the in-plane direction. This displacement, if part of an internal torsional motion, might very well account for the difference from the other structures. Similar torsional modes are not possible in the closed-ring structures and erythritol was studied at a significantly lower temperature than xylitol and MAHS, thus reducing the amplitude of such low-frequency modes.[3]

Two pyranosides were included in the analysis. The negative in-plane vibrations for the hydroxy groups in these structures are definitely a consequence of an overestimated libration perpendicular to the plane of the pyranose ring. Apart from this, the results are in accordance with those for the remaining structures.

4.2. Systems with short hydrogen bonds

The H atoms in the succinate and maleate ions in methylammonium hydrogen succinate monohydrate (MAHS; Flensburg *et al.*, 1995), methylammonium hydrogen maleate (MADMA; Madsen *et al.*, 1998) and sodium hydrogen maleate trihydrate (SHMAT; Olovsson *et al.*, 1984) involved in very short hydrogen bonds are very different from H atoms in normal hydroxy groups. We find generally the bond-directed MSD to be at least twice as large as seen for normal hydroxy groups, Table 8 and Fig. 6. The larger vibrations are in accordance with spectroscopic observations. Typical O—H

[3] Gao *et al.* (1994) report the torsional librations about C atoms in suberic acid to increase threefold upon going from 18.4 to 123 K.

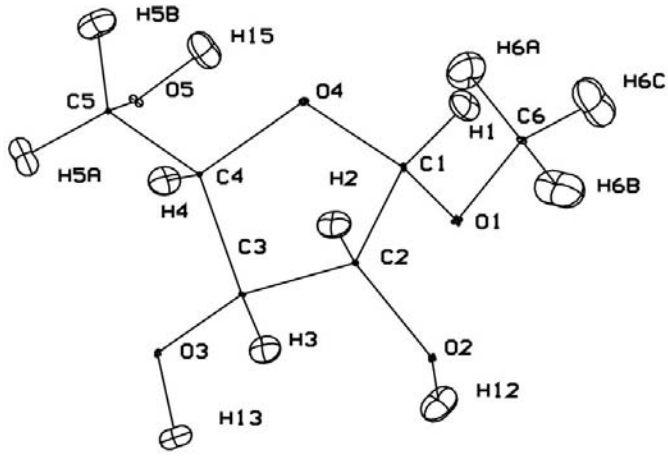

Figure 5
PEANUT (Hummel *et al.*, 1990) plot of the methyl α-D-xylofuranoside neutron experiment TLS refinement difference RMSD surface ($U_{obs} - U_{calc}$). RMSDs scaled up by 1.54.

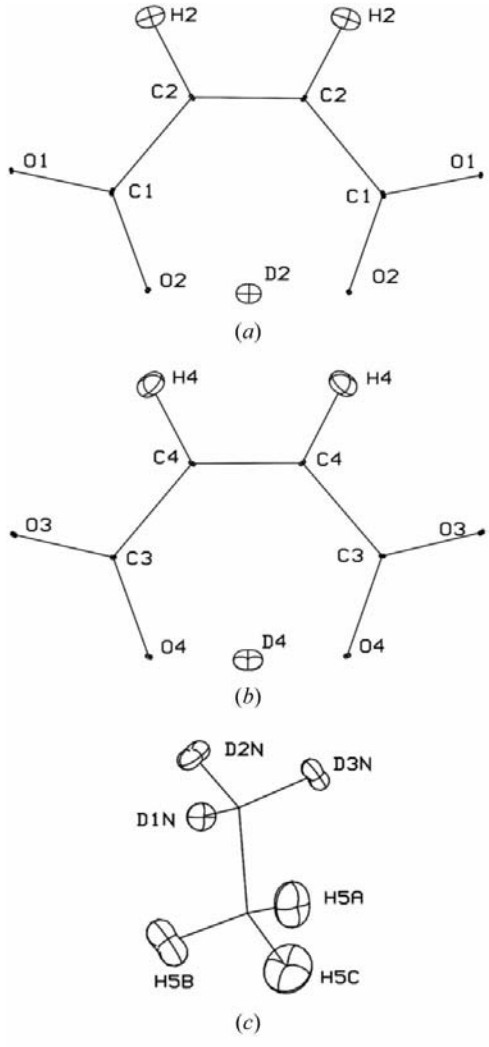

Figure 6
PEANUT (Hummel *et al.*, 1990) plot of methylammonium hydrogen maleate neutron experiment TLS refinement difference RMSD surface ($U_{obs} - U_{calc}$). RMSDs scaled up by 1.54.

Table 6
Analysis of the residual root-mean-square displacements (10^{-4} Å^2) from the TLS analysis of the erythritol (Ceccarelli *et al.*, 1980) neutron diffraction experiment.

The total and residual MSDs in the X—H direction and the U_{iso} value calculated as suggested by Stewart (1975) are listed in the section to the left. The eigenvalues of the residual MSD matrix are listed with the angle between the corresponding eigenvector and the closest axis in the local atomic coordinate system.

	Eigenvalues of the residual MSD matrix								
	$\langle\mu^2\rangle$ in X—H direction			Bond direction		Out-of-plane		In-plane	
	Residual	Total	U_{iso}	Angle	Value	Angle	Value	Angle	Value
H1*A*	59 (5)	115	192	5.9	58	3.4	131	6.3	196
H1*B*	50 (7)	107	188	6.9	48	9.8	138	12.0	181
H2	73 (5)	117	168	13.1	70	30.3	136	29.2	120
H11	47 (6)	118	184	6.5	46	13.2	174	11.5	107
H12	23 (6)	88	163	10.2	20	30.6	176	30.1	95

Table 7
Analysis of the residual root-mean-square displacements (10^{-4} Å^2) from the TLS analysis of the methyl α-D-xylofuranoside neutron diffraction experiment (Evdokimov *et al.*, 2001).

The total and residual MSDs in the X—H direction and U_{iso} values calculated as suggested by Stewart (1975) are listed in the section to the left. The eigenvalues of the residual MSD matrix are listed with the angle between the corresponding eigenvector and the closest axis in the local atomic coordinate system. Analysis of residual root-mean-square displacements from a TLS analysis of the methyl α-D-xylofuranoside neutron diffraction experiment (Evdokimov *et al.*, 2001).

				Eigenvalues of the residual MSD matrix					
	$\langle\mu^2\rangle$ in X—H direction			Bond direction		Out-of-plane		In-plane	
	Residual	Total	U_{iso}	Angle	Value	Angle	Value	Angle	Value
H1	38 (8)	98	174	11.1	34	24.2	136	21.5	162
H2	37 (11)	90	160	13.8	32	40.8	164	43.3	111
H3	50 (10)	102	159	9.9	48	42.9	141	43.9	103
H4	66 (10)	125	178	27.4	52	38.7	120	26.9	147
H5*A*	35 (9)	111	189	8.0	33	19.1	128	17.5	221
H5*B*	57 (12)	124	209	12.1	50	4.4	143	11.8	213
H15	71 (10)	146	206	27.0	59	8.3	222	27.8	113
H13	45 (13)	107	185	7.9	43	44.4	153	43.7	123
H12	34 (11)	117	185	13.7	28	9.1	234	13.7	120
H6*A*	57 (14)	143	264	17.2	42	3.3	305	17.5	209
H6*B*	47 (14)	131	273	4.0	47	0.7	413	4.0	158
H6*C*	49 (10)	164	274	5.0	47	4.0	405	3.8	162

Table 8
Analysis of the residual root-mean-square displacements (10^{-4} Å^2) from the TLS analysis of the maleate ion in the methylammonium hydrogen maleate neutron diffraction experiment (Madsen *et al.* 1998).

The total and residual MSDs in the X—H direction and the U_{iso} calculated as suggested by Stewart (1975) are listed in the section to the left. The eigenvalues of the residual MSD matrix are listed with the angle between the corresponding eigenvector and the closest axis in the local atomic coordinate system.

				Eigenvalues of the residual MSD matrix					
	$\langle\mu^2\rangle$ in X—H direction			Bond direction		Out-of-plane		In-plane	
	Residual	Total	U_{iso}	Angle	Value	Angle	Value	Angle	Value
H2	44 (26)	354	396	10.2	41	5.2	188	9.4	131
D2	94 (30)	271	277	3.5	95	15.2	10	15.0	54
H4	66 (18)	334	352	33.7	53	47.1	93	37.9	154
D4	136 (30)	269	276	2.2	136	28.3	1	28.4	72
H5*A*	92 (22)	425	443	20.1	55	22.8	224	30.3	369
H5*B*	68 (23)	446	475	13.2	49	15.9	260	18.4	435
H5*C*	78 (26)	466	508	24.6	17	30.2	364	22.2	462
D1*N*	34 (13)	307	311	12.4	30	8.9	147	14.6	125
D2*N*	26 (14)	315	330	16.7	10	30.1	122	34.5	225
D3*N*	42 (13)	317	324	15.1	31	43.4	204	44.0	105

stretching frequencies of the hydroxy groups involved in these very strong hydrogen bonds are 750–1000 cm^{-1} (Jeffrey, 1997). Similar O—D frequencies are about 550–730 cm^{-1}. This corresponds to MSDs in the range 0.024–0.018 Å^2 and 0.017–0.013 Å^2, respectively. The residual MSD for MAHS [0.0204 (47) Å^2] is thus close to the expected value, while the other results [MADMA: 0.094 (30) and 0.0136 (30) Å^2; SHMAT: 0.0121 (6) Å^2] are slightly lower than the expected values.

4.3. Methylammonium ions and water molecules

These entities, found in MADMA, MAHS and SHMAT, cannot be analyzed with a TLS model, because there are too few non-H atoms. Still, it is desirable to be able to assign ADPs to the H atoms in these entities also. Instead we have considered the H atoms as 'riding' on the atom they are bonded to (Busing & Levy, 1964) and subtracted the full MSD of the non-H atom. The resulting residual MSD matrices have been analyzed in the same way as the other H atoms. It is obvious that libration about the C—N axes in the methyl groups is not part of the riding motion and will be part of the residual MSDs. Indeed, rather large differences are seen between the out-of-plane vibrations of the methyl groups in MAHS and the furanosides. The most conspicuous differences are the in-plane vibrations which are much higher for the methylammonium ion in MADMA than for the other methyl groups.

5. Discussion and conclusions

We have obtained a satisfactory set of nuclear parameters for crystalline xylitol at 122.4 K, suitable for a combined neutron and X-ray diffraction study of the charge density of xylitol.

The analysis of internal mean-square displacements of the H atoms in xylitol gave very similar values for chemically equivalent H atoms. In the

nine low-temperature neutron studies subsequently analyzed, deviations between the different structures seem to reflect deficiencies in the rigid-body models. Without exception the smallest eigenvalue of the internal MSD matrix corresponds to the eigenvector closest to the bond direction. These eigenvalues match closely the spectroscopic stretching frequencies. The analysis shows that the use of an isotropic description of the H-atom displacement considerably overestimates the bond-directed MSD.

These results can be useful in the analysis of charge densities in organic molecular crystals on the basis of X-ray diffraction experiments alone. Most of the electron density associated with the H atoms in molecular crystals is located in the covalent X—H bonds. A good estimate of the bond-directed MSD is thus much more important than the estimate in any other direction. This study has shown that it is indeed possible to obtain a good estimate of the bond-directed MSD for H atoms if a reliable rigid-body model is available. We believe that the assignment of hydrogen MSDs depends first and foremost on the quality and validity of the rigid-body model and that the assignment of internal displacements based on spectroscopic values or rigid-body analysis of similar compounds provides a sufficient improvement to the models. The procedure seems to be a promising alternative to the refinement of isotropic displacement parameters.

APPENDIX *A*
From normal-mode frequencies to mean-square displacements

The result of the frequency calculation performed with *Gaussian*98 (Frisch *et al.*, 1998) is a set of molecular vibrational frequencies and the corresponding eigenvectors of displacement, along with the reduced mass of the corresponding harmonic oscillator. This allows the calculation of $\langle\mu^2\rangle$ for the harmonic oscillators using (1).

The eigenvectors are expressed in a Cartesian coordinate system, mass adjusted and normalized. The symmetric 3×3 matrix of the mean-square displacement amplitudes for atom k in mode j may be calculated on the basis of the 3-vector $\mathbf{e}(k|j)$ relating to this atom in the overall eigenvector. The total mean square displacement matrix is obtained by summation over all $3n - 6$ modes,[4]

$$\mathbf{U}(k) = \sum_j \langle u^2\rangle_j \mathbf{e}(k|j)[\mathbf{e}(k|j)]^T. \qquad (2)$$

These anisotropic displacement parameters correspond to the geometry optimized molecule, and are not directly transferable to the crystal geometry, because several of the C—C—O—H torsion angles change considerably upon geometry optimization.

[4] n is the number of atoms. The six lowest eigenmodes correspond to the overall translation and libration of the molecule and are not considered.
[5] The columns of this matrix are the 3-tuples that express the local basis in the global coordinate system.

Suppose $\mathbf{P}$ is the matrix that transforms a vector from the *global* Cartesian coordinate system to the *geometry optimized local* atomic coordinate system[5] defined as in §3.2. Likewise, let $\mathbf{O}$ be the matrix that transforms from the global coordinate system to a local atomic coordinate system in the *crystal geometry*. Since the symmetric mean-square displacement matrix $\mathbf{U}(k)$ of atom k corresponds to a linear transformation it can be expressed relative to the bases of the local atomic coordinate systems as $\mathbf{P}^{-1}\mathbf{U}(k)\mathbf{P}$ and $\mathbf{O}^{-1}\mathbf{U}(k)\mathbf{O}$, respectively. The atomic mean-square displacement matrices may therefore be transformed to correspond to the crystal geometry expressed in the *global* coordinate system by

$$\mathbf{U}_{\rm cr}(k) = \mathbf{O}\mathbf{P}^{-1}\mathbf{U}_{\rm opt}(k)\mathbf{P}\mathbf{O}^{-1}, \qquad (3)$$

where $\mathbf{U}_{\rm cr}(k)$ and $\mathbf{U}_{\rm opt}(k)$ are the mean-square displacement matrix (in the Cartesian global coordinate system) corresponding to the crystal and optimized geometries, respectively.

The $\mathbf{U}(k)$ matrix is normally expressed in the possibly oblique coordinate system defined by the unit-cell axis. This transformation is performed subsequently.

APPENDIX *B*
Definition of refinement statistics for the TLS analysis

Defined as in the *THMA*11 program (Schomaker & Trueblood, 1968),

$$wR^2(U_{ij}) = \left(\sum_{i,j,k}(w\Delta U_{ij})^2 / \sum_{i,j,k}(wU_{ij}^{\rm obs})^2\right)^{1/2},$$

$$wR^2(U_{ii}) = \left(\sum_{i,k}(w\Delta U_{ii})^2 / \sum_{i,k}(wU_{ii}^{\rm obs})^2\right)^{1/2},$$

$$\text{r.m.s.}(w\Delta U) = \left(\sum_{i,j,k}(w\Delta U_{ij})^2/w^2\right)^{1/2},$$

$$\text{e.s.d.}(w\Delta U) = \left(\sum_{i,j,k}(w\Delta U_{ij})^2/(n-p)\right)^{1/2}\left(6N_{\rm atoms}/w^2\right),$$

where n, p is the number of observations and parameters, respectively, and $N_{\rm atoms}$ is the number of atoms k used in the refinement.

We thank Garry McIntyre and Henning Osholm Sørensen for helpful discussions.

References

Becker, P. J. & Coppens, P. (1975). *Acta Cryst.* A**30**, 129–147.
Blessing, R. H. (1987). *Cryst. Rev.* **1**, 3–58.
Busing, W. R. & Levy, H. A. (1964). *Acta Cryst.* **17**, 142.
Capelli, S. C., Förtsch, M. & Bürgi, H. (2000). *Acta Cryst.* A**56**, 413–424.

Ceccarelli, C., Jeffrey, G. A. & McMullan, R. K. (1980). *Acta Cryst.* B**36**, 3079–3083.
Chen, L. & Craven, B. (1995). *Acta Cryst.* B**51**, 1081–1097.
Coppens, P., Guru Row, T. N., Leung, P., Stevens, E. D., Becker, P. J. & Yang, Y. W. (1979). *Acta Cryst.* A**35**, 63–72.
Coppens, P., Leiserowitz, L. & Rabinovish, D. (1965). *Acta Cryst.* **18**, 1035–1038.
Destro, R. & Merati, F. (1995). *Acta Cryst.* B**51**, 559–570.
Dunitz, J. D., Schomaker, V. & Trueblood, K. N. (1988). *J. Phys. Chem.* **92**, 856–867.
Evdokimov, A., Gilboa, A. J., Koetzle, T. F., Klooster, W. T., Schultz, A. J., Mason, S. A., Albinati, A. & Frolow, F. (2001). *Acta Cryst.* B**57**, 213–220.
Filhol, A. (1987). ILL Internal Report 87FI19T. ILL, Grenoble, France.
Flaig, R., Koritsanszky, T., Zobel, D. & Luger, P. (1998). *J. Am. Chem. Soc.* **120**, 2227–2238.
Flensburg, C., Larsen, S. & Stewart, R. F. (1995). *J. Phys. Chem.* **99**, 10130–10141.
Frisch, M. J., Trucks, G. W., Schlegel, H. B., Scuseria, G. E., Robb, M. A., Cheeseman, J. R., Zakrzewski, V. G., Montgomery, Jr, J. A., Stratmann, R. E., Burant, J. C., Dapprich, S., Millam, J. M., Daniels, A. D., Kudin, K. N., Strain, M. C., Farkas, O., Tomasi, J., Barone, V., Cossi, M., Cammi, R., Mennucci, B., Pomelli, C., Adamo, C., Clifford, S., Ochterski, J., Petersson, G. A., Ayala, P. Y., Cui, Q., Morokuma, K., Malick, D. K., Rabuck, A. D., Raghavachari, K., Foresman, J. B., Cioslowski, J., Ortiz, J. V., Baboul, A. G., Stefanov, B. B., Liu, G., Liashenko, A., Piskorz, P., Komaromi, I., Gomperts, R., Martin, R. L., Fox, D. J., Keith, T., Al-Laham, M. A., Peng, C. Y., Nanayakkara, A., Gonzalez, C., Challacombe, M., Gill, P. M. W., Johnson, B., Chen, W. W., Wong, M., Andres, J. L., Gonzalez, C., Head-Gordon, M. & Replogle, E. S. A. P. J. (1998). *Gaussian*98, Revision a.7. Gaussian, Inc., Pittsburgh, PA, USA.
Gao, Q., Weber, H.-P., Craven, B. M. & McMullan, R. K. (1994). *Acta Cryst.* B**50**, 695–703.
Higgs, P. W. (1955). *Acta Cryst.* **8**, 99–104.
Hirshfeld, F. L. & Hope, H. (1980). *Acta Cryst.* B**36**, 406–415.
Hummel, W., Hauser, J. & Buergi, H.-B. (1990). *J. Mol. Graph.* **8**, 214–220.
Jeffrey, G. A. (1990). *Acta Cryst.* B**46**, 89–103.
Jeffrey, G. A. (1997). *An Introduction to Hydrogen bonding*. Oxford University Press.
Jeffrey, G. A., Robbins, A., McMullan, R. K. & Takagi, S. (1980). *Acta Cryst.* B**36**, 373–377.
Johnson, C. K. (1970). *Generalized Treatments for Thermal Motion*, ch. 9. Oxford University Press.
Johnson, C. K. (1976). *ORTEP*II. Report ORNL-5138. Oak Ridge National Laboratory, Tennessee, USA.
Kampermann, S. P., Sabine, T. M., Craven, B. M. & McMullan, R. K. (1995). *Acta Cryst.* A**51**, 489–497.
Kim, H. S. & Jeffrey, G. A. (1969). *Acta Cryst.* B**25**, 2607–2613.
Luo, J., Ruble, J. R., Craven, B. M. & McMullan, R. K. (1996). *Acta Cryst.* B**52**, 357–368.
Madsen, D., Flensburg, C. & Larsen, S. (1998). *J. Phys. Chem. A*, **102**, 2177–2188.
Olovsson, G., Olovsson, I. & Lehmann, M. S. (1984). *Acta Cryst.* C**40**, 1521–1526.
Panagiotopoulos, N. C., Jeffrey, G. A., La Placa, S. J. & Hamilton, W. C. (1974). *Acta Cryst.* B**30**, 1421–1430.
Park, J. Y. & Jeffrey, G. A. (1971). *Acta Cryst.* B**27**, 2393–2401.
Rosenfield, R. E. Jr & Trueblood, K. N. & Dunitz, J. D. (1978). *Acta Cryst.* A**34**, 828–829.
Rousseau, B., van Alsenoy, C., Keuleers, R. & Desseyn, H. O. (1998). *J. Phys. Chem. A*, **102**, 6540–6548.
Schomaker, V. & Trueblood, K. N. (1968). *Acta Cryst.* B**24**, 63–76.
Schomaker, V. & Trueblood, K. N. (1998). *Acta Cryst.* B**54**, 507–514.
Sears, V. F. (1992). *Neutron News*, **3**, 26–27.
Sheldrick, G. M. (1990). *Acta Cryst.* A**46**, 467–473.
Stewart, R. F. (1975). *Acta Cryst.* A**32**, 182–185.
Stewart, R. F., Davidson, E. R. & Simpson, W. T. (1965). *J. Chem. Phys.* **42**, 3175–3187.
Stewart, R. F., Spackman, M. A. & Flensburg, C. (1998). *VALRAY*98 *User's Manual*. Carnegie-Mellon University, USA, and University of Copenhagen, Denmark.
Weber, H.-P., Craven, B. M., Sawzip, P. & McMullan, R. K. (1991). *Acta Cryst.* B**47**, 116–127.
Wilkinson, C., Khamis, H. W., Stansfield, R. F. D. & McIntyre, G. J. (1988). *J. Appl. Cryst.* **21**, 471–478.
Willis, B. T. M. & Pryor, A. W. (1975). *Thermal Vibrations in Crystallography*. Cambridge University Press.